Available online at www.sciencedirect.com
SCIENCE DIRECT
Journal of Sound and Vibration 295 (2006) 1044–1059
JOURNAL OF SOUND AND VIBRATION
www.elsevier.com/locate/jsvi

Exact natural frequencies of a three-dimensional shear–torsion beam with doubly asymmetric cross-section using a two-dimensional approach

B. Rafezy[a,b], W.P. Howson[a,*]

[a]*Cardiff School of Engineering, Cardiff University, The Parade, Cardiff CF24 3AA, UK*
[b]*Sahand University of Technology, P.O. Box 51335/1996, Tabriz, Iran*

Received 1 August 2005; received in revised form 7 February 2006; accepted 14 February 2006
Available online 24 May 2006

Abstract

This paper presents an exact analytical approach to the calculation of the natural frequencies of structures comprising contiguous, three-dimensional shear–torsion beams with doubly asymmetric cross-section. Such component members have the unusual theoretical property that they allow for coupled torsional and shearing deformation, but not bending deformation. Initially, exact dynamic member stiffness matrices (exact finite elements) are developed for planar shear and torsional motion. These matrices can be combined in the usual way to model stepped and continuous beams whose uncoupled frequencies can then be determined exactly. It is then shown how the corresponding coupled frequencies can be established easily from the uncoupled values through an exact relationship. This enables coupled, three-dimensional vibration problems to be solved very efficiently using a two-dimensional approach. The paper is concluded with an example that clarifies the theory, together with a parametric study that enables guidance to be given as to when lateral–torsional coupling may safely be ignored.

1. Introduction

Matrix methods of solving problems in dynamics emerged to prominence in the late 1960s. One of the first papers to describe the formulation of a dynamic stiffness matrix was presented by Laursen et al. [1]. Initially attention is focused on the development of the individual member matrix, which relates the amplitudes of the sinusoidally varying moment and shear forces at the end of a beam member to the corresponding displacements. Subsequently it is shown how these matrices can be formed into an overall dynamic stiffness matrix for a structure. Cheng [2] and Wang and Kinsman [3] subsequently developed the dynamic stiffness matrix for a Timoshenko beam. Later Howson and Williams [4] derived the dynamic stiffness matrix of an axially loaded Timoshenko beam that has been used extensively in the eigensolution of plane frames [5–7].

*Corresponding author. Tel.: +44 2920 874263; fax: +44 2920 874597.
E-mail address: howson@cf.ac.uk (W.P. Howson).

0022-460X/$ - see front matter © 2006 Published by Elsevier Ltd.
doi:10.1016/j.jsv.2006.02.007

In the last two decades, research on the dynamic stiffness matrix formulation for beams has grown enormously and now encompasses theory for beams on elastic foundations [8–10], tapered beams [11] and curved beams [9,12–15]. However, a progressively more important area of interest is the bending–torsion coupled beam. In these beams the elastic centre and the centre of mass are not coincident, so the translational and torsional modes are inherently coupled as a result of this offset. The solution for individual beams has been approached in different ways by Gere and Lin [16], Falco and Gasparetto [17] and Dokumaci [18]. However, development of the dynamic stiffness matrix for such beams is relatively new and has been considered by only a few investigators. Hallauer and Liu [19] derived the exact dynamic stiffness matrix for a straight, bending–torsion beam using Euler–Bernoulli–Saint Venant theory, but restricted the bending translation to a single plane. Friberg [20] used the same theory to formulate the equivalent 12×12 matrix for translation in two orthogonal planes. He later [21] included the effect of axial load and warping rigidity using Vlasov's torsion theory and developed the 14×14 dynamic stiffness matrix numerically. On the other hand, Banerjee [22] derived explicit expressions for the stiffness elements and later included the effects of shear deformation and rotary inertia [23]. Subsequently, Banerjee et al. [24] studied the vibration of a bending–torsion beam with singly asymmetric cross-section, including warping rigidity and showed that large errors may be incurred in the calculation of natural frequencies of thin walled open section beam assemblies when the effect of warping is ignored. In a recent paper Rafezy and Howson [25] considered the vibration analysis of three-dimensional shear–torsion beams with doubly asymmetric cross-section and derived a 6×6 dynamic stiffness matrix. Such beams have the unusual theoretical property that they allow for coupled torsional and shearing deformation, but not bending deformation. This approach can be used very efficiently in the approximate determination of the lower natural frequencies of three-dimensional, multi-storey framed structures [26,27], including those that are doubly asymmetric on plan.

This paper extends the work of Rafezy and Howson [25] by simplifying the method for calculating the exact, coupled natural frequencies of three-dimensional shear–torsion beams with doubly asymmetric cross-section. As in the previous paper [25], this formulation finds considerable application in the approximate analysis of asymmetric, three-dimensional frame structures and yields a particularly simple hand method when the properties of the structure are uniform throughout its height.

The paper comprises three main parts. Initially the governing differential equations are formulated for uncoupled, planar shear and torsion using a continuum approach. The equations are solved and posed in the form of two dimensional, exact member stiffness matrices (exact finite elements) that can be assembled in the usual way to form any permissible structure. Such a formulation accounts for the uniform distribution of mass in the member and necessitates the solution of a transcendental eigenvalue problem. This is achieved using the Wittrick–Williams algorithm. The corresponding equations for coupled motion in three dimensions are then presented and solved once more in the form of a dynamic stiffness matrix. This matrix itself could be used to calculate the coupled natural frequencies of an individual member or any appropriate structure comprising such members. However, a simpler method is then proposed in which the shear–torsion members of the structure are replaced in turn by their uncoupled counterparts. This enables the exact uncoupled frequencies to be determined, from which the corresponding coupled frequencies can be evaluated in a simple way through an exact relationship. Finally, an example is given to clarify the theory, together with a parametric study that investigates the effect of cross-sectional asymmetry and the ratio of torsional to translational rigidity on the vibrational behaviour of a shear cantilever. Guidance is then given as to when lateral–torsional coupling may safely be ignored.

2. Dynamic member stiffness matrix for a two-dimensional shear beam and torsion beam

Fig. 1 depicts a shear beam of length L whose longitudinal, mass and elastic axes all coincide with the z axis. By definition the beam is only allowed to undergo shear deformation in the x–z and y–z planes. In similar fashion, Fig. 2 depicts a torsion beam that can only rotate in torsion about its longitudinal axis, thus confining rotation to the x–y plane. All degrees of freedom are uncoupled and the motion in the three planes can therefore be dealt with separately. Assuming harmonic motion, Fig. 1(a) depicts the amplitudes of the nodal forces and displacements when the beam is undergoing shear vibration in the x–z (y–z) plane and Fig. 1(b)

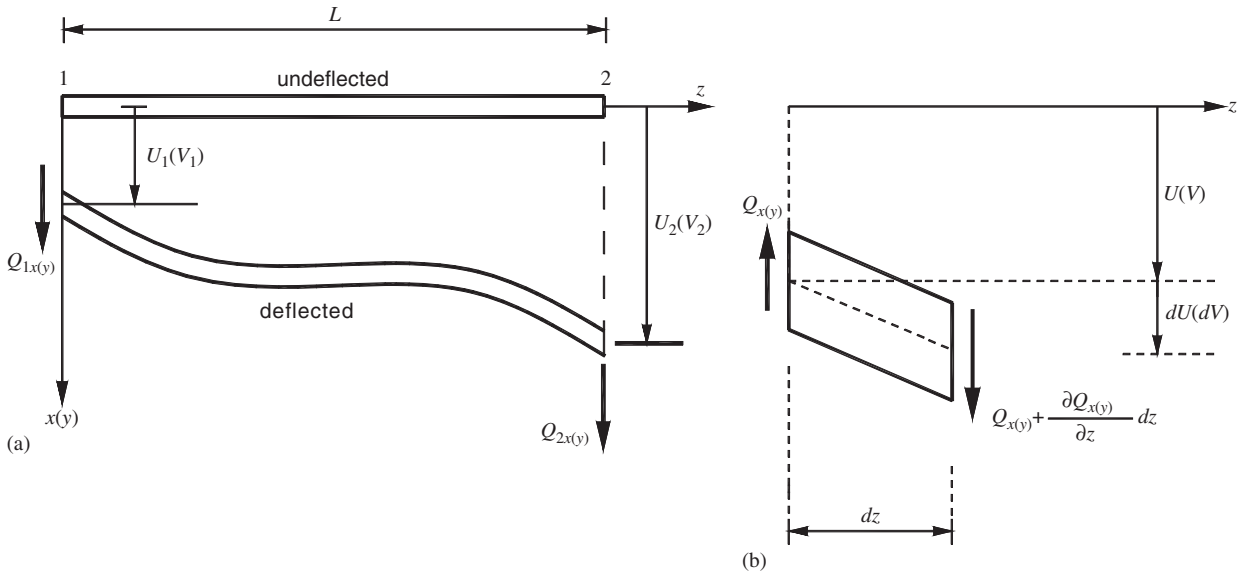

Fig. 1. Coordinate system and positive sign convention of a two-dimensional shear beam in the local x–z (y–z) plane: (a) amplitudes of nodal forces and displacements; (b) amplitudes of forces and displacements associated with an elemental length of the beam.

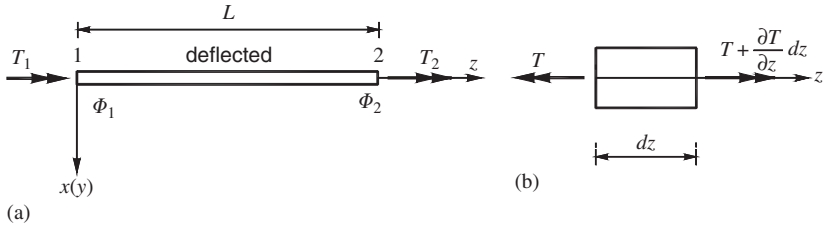

Fig. 2. Coordinate system and positive sign convention of a two-dimensional torsion beam subjected to pure torsion in the x–y plane: (a) amplitudes of nodal forces and displacements; (b) amplitudes of forces associated with an elemental length of the beam.

shows the corresponding forces and displacements associated with an elemental length of the member. Figs. 2(a) and (b) show the corresponding terms for the case of torsion.

Thus equating the resultant force on an element to the corresponding mass acceleration in each of the three cases gives

$$\frac{\mathrm{d}Q_x(z)}{\mathrm{d}z} = -m\omega^2 U(z), \quad \frac{\mathrm{d}Q_y(z)}{\mathrm{d}z} = -m\omega^2 V(z) \quad \text{and} \quad \frac{\mathrm{d}T(z)}{\mathrm{d}z} = -r_m^2 m\omega^2 \Phi(z), \tag{1a–c}$$

where $Q_x(z)$, $U(z)$ and $Q_y(z)$, $V(z)$ are the amplitudes of the shear force and lateral displacement in the x–z and y–z planes, respectively; $T(z)$, $\Phi(z)$ are the corresponding terms for torsion in the x–y plane, m is the uniformly distributed mass/unit length of the beam; ω is the circular frequency and r_m is the polar mass radius of gyration of the cross-section. Finally, the constitutive relationships for shear and torsion give

$$Q_x(z) = GA_x \frac{\mathrm{d}U(z)}{\mathrm{d}z}, \quad Q_y(z) = GA_y \frac{\mathrm{d}V(z)}{\mathrm{d}z} \quad \text{and} \quad T(z) = GJ \frac{\mathrm{d}\Phi(z)}{\mathrm{d}z}, \tag{2a–c}$$

where GA_x, GA_y and GJ are the shear and torsional rigidities in the x–z, y–z and x–y planes, respectively.

Introducing the non-dimensional parameter

$$\xi = z/L \tag{3}$$

enables Eqs. (2) to be written as

$$Q_x(\xi) = k_x DU(\xi), \quad Q_y(\xi) = k_y DV(\xi) \quad \text{and} \quad T(\xi) = k_\varphi D\Phi(\xi), \tag{4a–c}$$

where

$$D = \frac{\mathrm{d}}{\mathrm{d}\xi}, \quad k_x = GA_x/L, \quad k_y = GA_y/L, \quad \text{and} \quad k_\varphi = GJ/L. \tag{5a–c}$$

Due to the similarity of Eqs. (4) they may all be written as

$$F(\xi) = kDW(\xi), \tag{6}$$

where

$$F(\xi) = Q_x(\xi),\ Q_y(\xi) \text{ or } T(\xi),$$

$$k = k_x,\ k_y \text{ or } k_\varphi$$

and

$$W(\xi) = U(\xi),\ V(\xi) \text{ or } \Phi(\xi). \tag{7}$$

In similar fashion, combining the corresponding parts of Eqs. (1) and (2) yields the required governing differential equations of motion in the three planes as

$$(D^2 + \omega^2\lambda_x^2)U(\xi) = 0, \quad (D^2 + \omega^2\lambda_y^2)V(\xi) = 0 \quad \text{and} \quad (D^2 + \omega^2\lambda_\varphi^2)\Phi(\xi) = 0, \tag{8a–c}$$

where

$$\lambda_x^2 = mL^2/GA_x, \quad \lambda_y^2 = mL^2/GA_y \quad \text{and} \quad \lambda_\varphi^2 = r_m^2 mL^2/GJ. \tag{9a–c}$$

Once more due to the similarity of Eqs. (8) they may all be written as

$$(D^2 + \omega^2\lambda^2)W(\xi) = 0, \quad \text{where } \lambda = \lambda_x, \quad \lambda_y \text{ or } \lambda_\varphi \tag{10}$$

depending on the expression for $W(\xi)$.

The solution to Eq. (10) can be found by substituting the trial solution $W(\xi) = e^{s\xi}$, which yields the characteristic equation

$$s^2 + \lambda^2\omega^2 = 0, \tag{11}$$

with the result that

$$s = \pm \mathrm{i}\lambda\omega, \quad \text{where } \mathrm{i} = \sqrt{-1}. \tag{12}$$

It follows that the general solution of Eq. (10) is of the form

$$W(\xi) = C_1 \cos\lambda\omega\xi + C_2 \sin\lambda\omega\xi. \tag{13}$$

In turn, the expression for the force $F(\xi)$ can be obtained from Eq. (6) as

$$F(\xi) = k(-C_1\lambda\omega \sin\lambda\omega\xi + C_2\lambda\omega \cos\lambda\omega\xi). \tag{14}$$

The nodal displacements and forces at each end of the beam, based on the sign conventions of Figs. 1 and 2, are, respectively,

$$\text{At node 1 } (\xi = 0) \quad W = W_1, \quad F = -F_1, \tag{15}$$

$$\text{At node 2 } (\xi = 1) \quad W = W_2, \quad F = F_2. \tag{16}$$

Substituting Eqs. (15) and (16) into Eq. (13) gives

$$\begin{bmatrix} C_1 \\ C_2 \end{bmatrix} = \frac{1}{\sin\lambda\omega} \begin{bmatrix} \sin\lambda\omega & 0 \\ -\cos\lambda\omega & 1 \end{bmatrix} \begin{bmatrix} W_1 \\ W_2 \end{bmatrix} \tag{17}$$

and

$$\begin{bmatrix} F_1 \\ F_2 \end{bmatrix} = k \begin{bmatrix} 0 & -\lambda\omega \\ -\lambda\omega \sin \lambda\omega & \lambda\omega \cos \lambda\omega \end{bmatrix} \begin{bmatrix} C_1 \\ C_2 \end{bmatrix}. \tag{18}$$

Combining Eqs. (17) and (18) gives

$$\begin{bmatrix} F_1 \\ F_2 \end{bmatrix} = \frac{k\lambda\omega}{\sin \lambda\omega} \begin{bmatrix} \cos \lambda\omega & -1 \\ -1 & \cos \lambda\omega \end{bmatrix} \begin{bmatrix} W_1 \\ W_2 \end{bmatrix} \tag{19}$$

or

$$\mathbf{f} = \mathbf{kd}, \tag{20}$$

where $\mathbf{k}$ is the required dynamic stiffness matrix for uncoupled shear or torsion of the beam.

3. Wittrick–Williams algorithm

The dynamic structure stiffness matrix, $\mathbf{K}$, when assembled from the member stiffness matrices yields the required natural frequencies as solutions of the equation

$$\mathbf{KD} = \mathbf{0}, \tag{21}$$

where $\mathbf{D}$ is the vector of amplitudes of the harmonically varying nodal displacements and $\mathbf{K}$ is a function of ω, the circular frequency. When, as in this case, $\mathbf{K}$ is developed from exact member theory, the determinant is a highly irregular, transcendental function of ω and the difficulties involved in determining the required natural frequencies are well known [28]. However, it has been proven [29] that any required natural frequency can be converged upon to any desired accuracy with the certain knowledge that none have been missed by use of the Wittrick–Williams (W–W) algorithm [30,31], which states that

$$J = J_0 + s\{\mathbf{K}\}, \tag{22}$$

where J is the number of natural frequencies of the structure exceeded by some trial frequency, ω^*, J_0 is the number of natural frequencies that would still be exceeded if all members were clamped at their ends so as to make $\mathbf{D} = \mathbf{0}$ and $s\{\mathbf{K}\}$ is the sign count of the matrix $\mathbf{K}$. $s\{\mathbf{K}\}$ is defined in Ref. [31] and is equal to the number of negative elements on the leading diagonal of the upper triangular matrix obtained from $\mathbf{K}$, when $\omega = \omega^*$, by the standard form of Gauss elimination without row interchanges.

From the definition of J_0 it can be seen that [30,31]

$$J_0 = \sum J_m, \tag{23}$$

where J_m is the number of natural frequencies of a component member, with its ends clamped, which have been exceeded by ω^* and the summation extends over all members.

In the present case it is possible to determine the value of J_m for a member symbolically using a direct approach, as follows.

The end displacement conditions for a clamped–clamped member in a given plane are

$$\text{at node 1} \quad (\xi = 0) \quad W(0) = 0; \quad \text{at node 2} \quad (\xi = 1) \quad W(1) = 0. \tag{24}$$

Substituting Eq. (24) into Eq. (13) gives

$$C_1 = 0 \quad \text{and} \quad C_2 \sin \lambda\omega = 0, \tag{25}$$

which requires that $\lambda\omega = i\pi$ and hence

$$\omega = \frac{i\pi}{\lambda} \quad (i = 1, 2, 3, \ldots). \tag{26}$$

Thus J_m for any trial frequency ω^* is given by

$$J_m = \text{int}\left[\frac{\omega^*}{(\pi/\lambda)}\right], \tag{27}$$

in which int represents the image integer function, i.e. the greatest integer $<\omega^*/(\pi/\lambda)$.

4. Three-dimensional shear–torsion beam

Fig. 3 shows a uniform, three-dimensional shear–torsion beam of length L, with doubly asymmetric cross-section. The origin of the coordinate system is located at the shear centre S, with the result that the elastic axis coincides with the z-axis. Point C on the cross-section denotes the centre of mass and its location in the coordinate system Sxy is given by x_c and y_c. The resulting mass axis then runs parallel to the z-axis through x_c, y_c.

Rafezy and Howson [25] derived the governing differential equations of motion of such a beam as

$$U''(\xi) + \omega^2\lambda_x^2 U(\xi) - y_c\omega^2\lambda_x^2\Phi(\xi) = 0, \tag{28a}$$

$$V''(\xi) + \omega^2\lambda_y^2 V(\xi) + x_c\omega^2\lambda_y^2\Phi(\xi) = 0, \tag{28b}$$

$$\Phi''(\xi) - (1/r_m^2)y_c\omega^2\lambda_\varphi^2 U(\xi) + (1/r_m^2)x_c\omega^2\lambda_\varphi^2 V(\xi) + \omega^2\lambda_\varphi^2\Phi(\xi) = 0, \tag{28c}$$

in which $U(\xi)$, $V(\xi)$ and $\Phi(\xi)$ are the amplitudes of the sinusoidally varying displacements in the x, y and torsional directions, respectively, and

$$\lambda_x^2 = mL^2/GA_x, \quad \lambda_y^2 = mL^2/GA_y, \quad \lambda_\varphi^2 = r_m^2 mL^2/GJ \quad \text{and} \quad \xi = z/L, \tag{29a–d}$$

where GA_x and GA_y are the shear rigidities of the beam in the x and y directions, respectively, and GJ and r_m are the torsional rigidity and polar mass radius of gyration of the cross-section.

They proceeded to solve the equations and posed the solution in the form of a dynamic stiffness matrix which can be used directly for the frequency analysis of three-dimensional shear–torsion beams. Part of their solution is reproduced here as it is needed when deriving the new method based on a simpler, two-dimensional approach.

Rewriting Eqs. (28) in matrix form gives

$$\begin{bmatrix} D^2+\omega^2\lambda_x^2 & 0 & -y_c\omega^2\lambda_x^2 \\ 0 & D^2+\omega^2\lambda_y^2 & x_c\omega^2\lambda_y^2 \\ -(1/r_m^2)y_c\omega^2\lambda_\varphi^2 & (1/r_m^2)x_c\omega^2\lambda_\varphi^2 & D^2+\omega^2\lambda_\varphi^2 \end{bmatrix} \begin{bmatrix} U(\xi) \\ V(\xi) \\ \Phi(\xi) \end{bmatrix} = \mathbf{0}, \tag{30}$$

in which $D = \mathrm{d}/\mathrm{d}\xi$.

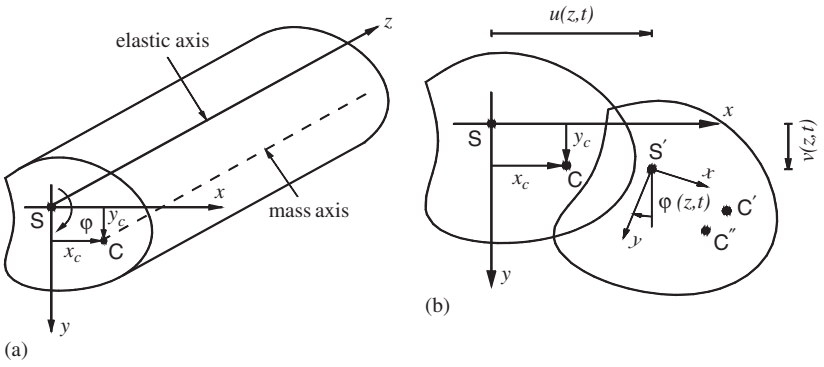

Fig. 3. (a) Coordinate system and notation for a three-dimensional, shear–torsion beam with doubly asymmetric cross-section; (b) typical displacement configuration of a cross-section.

Eq. (30) can be combined into one equation by eliminating either U, V or Φ to give the sixth-order differential equation

$$\begin{vmatrix} D^2+\omega^2\lambda_x^2 & 0 & -y_c\omega^2\lambda_x^2 \\ 0 & D^2+\omega^2\lambda_y^2 & x_c\omega^2\lambda_y^2 \\ -(1/r_m^2)y_c\omega^2\lambda_\varphi^2 & (1/r_m^2)x_c\omega^2\lambda_\varphi^2 & D^2+\omega^2\lambda_\varphi^2 \end{vmatrix} W(\xi)=0, \tag{31}$$

where $W = U$, V or Φ.

The general solution of Eq. (31) is found by substituting the trial solution $W(\xi)=e^{s\xi}$ to yield the characteristic equation

$$\begin{vmatrix} b^2+\lambda_x^2 & 0 & -y_c\lambda_x^2 \\ 0 & b^2+\lambda_y^2 & x_c\lambda_y^2 \\ -y_c\lambda_\varphi^2 & x_c\lambda_\varphi^2 & r_m^2(b^2+\lambda_\varphi^2) \end{vmatrix} = 0, \tag{32}$$

where $b^2=(s/\omega)^2$.

Eq. (32) is a cubic equation in the frequency parameter b^2 and it has been proven by Rafezy and Howson [25] that it always has three negative real roots. Let these three roots be $-b_1^2$, $-b_2^2$ and $-b_3^2$, where b_j^2 ($j=1,2,3$) are all real and positive. Therefore,

$$\left(\frac{s}{\omega}\right)^2 = -b_j^2 \quad \text{giving} \quad s=\pm \mathrm{i}\omega b_j \quad (j=1,2,3) \quad \text{where } \mathrm{i}=\sqrt{-1}. \tag{33}$$

It follows that the solution of Eq. (31) can be written in the form

$$W(\xi)=C_1\cos b_1\omega\xi + C_2\sin b_1\omega\xi + C_3\cos b_2\omega\xi + C_4\sin b_2\omega\xi + C_5\cos b_3\omega\xi + C_6\sin b_3\omega\xi. \tag{34}$$

Eq. (34) represents the solution for $U(\xi)$, $V(\xi)$ and $\Phi(\xi)$, since they are all related via Eq. (30). They can therefore be written individually as

$$U(\xi)=t_1^u(C_1\cos b_1\omega\xi + C_2\sin b_1\omega\xi)+t_2^u(C_3\cos b_2\omega\xi + C_4\sin b_2\omega\xi)+t_3^u(C_5\cos b_3\omega\xi + C_6\sin b_3\omega\xi), \tag{35a}$$

$$V(\xi)=t_1^v(C_1\cos b_1\omega\xi + C_2\sin b_1\omega\xi)+t_2^v(C_3\cos b_2\omega\xi + C_4\sin b_2\omega\xi)+t_3^v(C_5\cos b_3\omega\xi + C_6\sin b_3\omega\xi), \tag{35b}$$

$$\Phi(\xi)=C_1\cos b_1\omega\xi + C_2\sin b_1\omega\xi + C_3\cos b_2\omega\xi + C_4\sin b_2\omega\xi + C_5\cos b_3\omega\xi + C_6\sin b_3\omega\xi, \tag{35c}$$

in which the constants t_j^u and t_j^v ($j=1,2,3$) are given by

$$t_j^u=\frac{y_c\lambda_x^2}{\lambda_x^2-b_j^2} \quad \text{and} \quad t_j^v=\frac{-x_c\lambda_y^2}{\lambda_y^2-b_j^2} \quad (j=1,2,3). \tag{36a,b}$$

The corresponding forces can be retrieved from Eqs. (5)–(7) as

$$Q_x(z)=k_xDU(\xi), \quad Q_y(z)=k_yDV(\xi) \quad \text{and} \quad T(z)=k_\varphi D\Phi(\xi). \tag{37a−c}$$

The nodal forces and displacements can now be defined in the member co-ordinate system of Figs. 4(a) and (b), as follows:

$$\text{at } (\xi=0) \quad U=U_1, \quad V=V_1, \quad \Phi=\Phi_1, \quad Q_x=-Q_{1x}, \quad Q_y=-Q_{1y}, \quad T=-T_1, \tag{38a}$$

$$\text{at } (\xi=1) \quad U=U_2, \quad V=V_2, \quad \Phi=\Phi_2, \quad Q_x=Q_{2x}, \quad Q_y=Q_{2y}, \quad T=T_2. \tag{38b}$$

The nodal displacements can then be determined from Eqs. (35) as

$$\begin{bmatrix} \mathbf{d}_1 \\ \mathbf{d}_2 \end{bmatrix} = \begin{bmatrix} \mathbf{E} & \mathbf{0} \\ \mathbf{0} & \mathbf{E} \end{bmatrix} \begin{bmatrix} \mathbf{I} & \mathbf{0} \\ \mathbf{C} & \mathbf{S} \end{bmatrix} \begin{bmatrix} \mathbf{C}_o \\ \mathbf{C}_e \end{bmatrix} \tag{39}$$

or

$$\mathbf{d}=\mathbf{sc}, \tag{40}$$

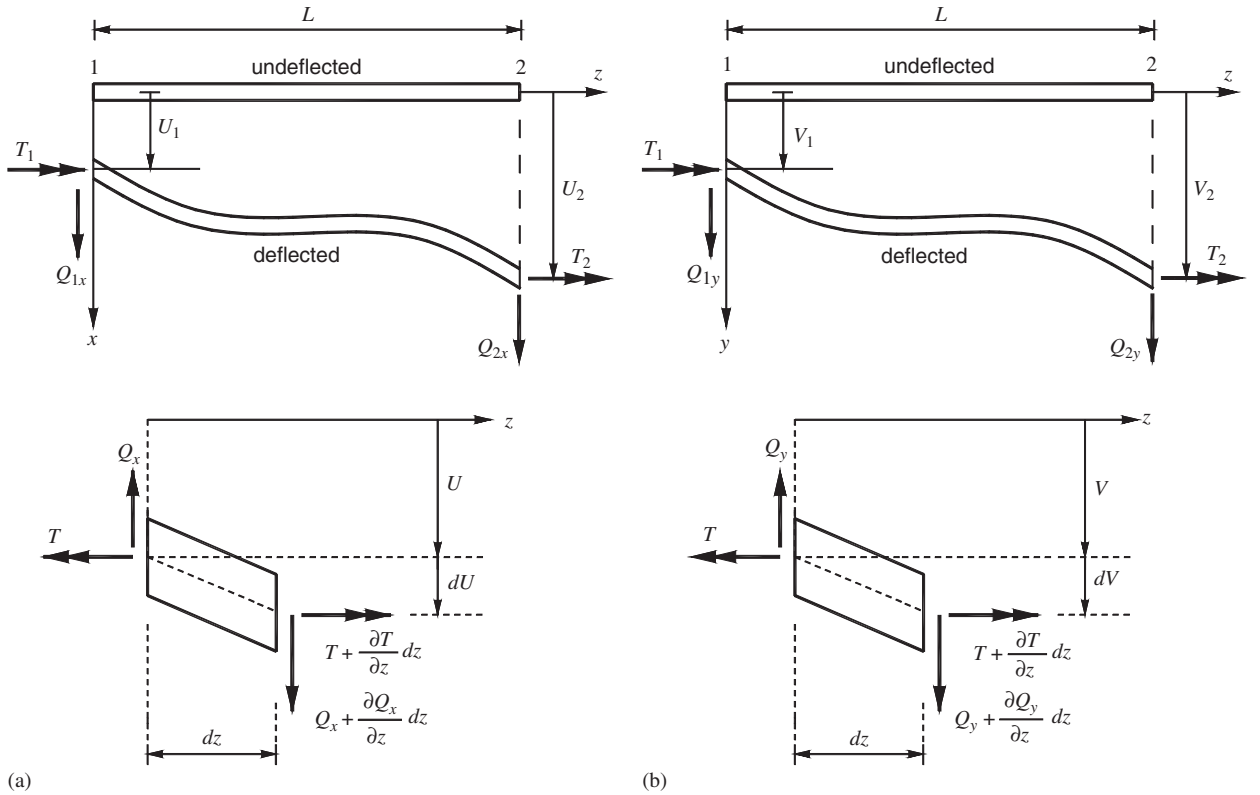

Fig. 4. End conditions for forces and displacements of a three-dimensional, doubly asymmetric shear beam: (a) sign convention for force and displacement for the shear beam in the x–z plane; (b) sign convention for force and displacement for the shear beam in the y–z plane.

where

$$\mathbf{d}_1=\begin{bmatrix}U_1\\V_1\\\Phi_1\end{bmatrix},\quad \mathbf{d}_2=\begin{bmatrix}U_2\\V_2\\\Phi_2\end{bmatrix},\quad \mathbf{C}_o=\begin{bmatrix}C_1\\C_3\\C_5\end{bmatrix},\quad \mathbf{C}_e=\begin{bmatrix}C_2\\C_4\\C_6\end{bmatrix},\quad \mathbf{E}=\begin{bmatrix}t_1^u & t_2^u & t_3^u\\ t_1^v & t_2^v & t_3^v\\ 1 & 1 & 1\end{bmatrix},$$

$$\mathbf{C}=\begin{bmatrix}C_{b_1\omega} & 0 & 0\\ 0 & C_{b_2\omega} & 0\\ 0 & 0 & C_{b_3\omega}\end{bmatrix},\quad \mathbf{S}=\begin{bmatrix}S_{b_1\omega} & 0 & 0\\ 0 & S_{b_2\omega} & 0\\ 0 & 0 & S_{b_3\omega}\end{bmatrix},$$

$$\mathbf{I}\text{ is the unit matrix},\quad S_{b_j\omega}=\sin b_j\omega\quad\text{and}\quad C_{b_j\omega}=\cos b_j\omega\quad(j=1,2,3).\tag{41}$$

Hence the vector of constants $[\mathbf{C}_o\ \ \mathbf{C}_e]^{\mathrm{T}}$ can be determined from Eq. (39) as

$$\begin{bmatrix}\mathbf{C}_o\\ \mathbf{C}_e\end{bmatrix}=\begin{bmatrix}\mathbf{I} & \mathbf{0}\\ \mathbf{C} & \mathbf{S}\end{bmatrix}^{-1}\begin{bmatrix}\mathbf{E} & \mathbf{0}\\ \mathbf{0} & \mathbf{E}\end{bmatrix}^{-1}\begin{bmatrix}\mathbf{d}_1\\ \mathbf{d}_2\end{bmatrix}.\tag{42}$$

In similar fashion the vector of nodal forces can be determined from Eqs. (37) as

$$\begin{bmatrix}\mathbf{p}_1\\ \mathbf{p}_2\end{bmatrix}=\begin{bmatrix}\mathbf{DEb} & \mathbf{0}\\ \mathbf{0} & \mathbf{DEb}\end{bmatrix}\begin{bmatrix}\mathbf{0} & -\mathbf{I}\\ -\mathbf{S} & \mathbf{C}\end{bmatrix}\begin{bmatrix}\mathbf{C}_o\\ \mathbf{C}_e\end{bmatrix},\tag{43}$$

or

$$\mathbf{p}=\mathbf{s}^*\mathbf{c},\tag{44}$$

where

$$\mathbf{p}_1 = \begin{bmatrix} Q_{1x} \\ Q_{1y} \\ T_1 \end{bmatrix}, \quad \mathbf{p}_2 = \begin{bmatrix} Q_{2x} \\ Q_{2y} \\ T_2 \end{bmatrix}, \quad \mathbf{D} = \omega \begin{bmatrix} k_x & 0 & 0 \\ 0 & k_y & 0 \\ 0 & 0 & k_\varphi \end{bmatrix} \quad \text{and} \quad \mathbf{b} = \begin{bmatrix} b_1 & 0 & 0 \\ 0 & b_2 & 0 \\ 0 & 0 & b_3 \end{bmatrix}. \tag{45}$$

Thus the required stiffness matrix can be developed by substituting Eqs. (42) into Eqs. (43) to give

$$\begin{bmatrix} \mathbf{p}_1 \\ \mathbf{p}_2 \end{bmatrix} = \begin{bmatrix} \mathbf{DEb} & \mathbf{0} \\ \mathbf{0} & \mathbf{DEb} \end{bmatrix} \begin{bmatrix} \mathbf{0} & -\mathbf{I} \\ -\mathbf{S} & \mathbf{C} \end{bmatrix} \begin{bmatrix} \mathbf{I} & \mathbf{0} \\ \mathbf{C} & \mathbf{S} \end{bmatrix}^{-1} \begin{bmatrix} \mathbf{E} & \mathbf{0} \\ \mathbf{0} & \mathbf{E} \end{bmatrix}^{-1} \begin{bmatrix} \mathbf{d}_1 \\ \mathbf{d}_2 \end{bmatrix} \tag{46}$$

or

$$\mathbf{p} = \mathbf{s}^* \mathbf{s}^{-1} \mathbf{d} = \mathbf{k}\mathbf{d}. \tag{47}$$

5. Equivalent two-dimensional approach

The dynamic stiffness relationship of Eq. (47) represents the exact solution of the simultaneous differential equations that were presented in Eq. (28) and which govern the motion of a three-dimensional shear–torsion beam with doubly asymmetric cross-section. It could therefore be used in the usual way to develop a model of any permissible structure, from which the natural frequencies could be determined using the W–W algorithm. There is, however, a very much easier way of evaluating precisely the same coupled natural frequencies using a simple two step procedure which is proven to be exact in the following section.

5.1. Analogous uncoupled system

The effect of setting x_c and y_c to zero in Eq. (31) is that the equations become decoupled with the result that they can be written in the following form:

$$(D^2 + \omega^2 \lambda_x^2) U(\xi) = 0, \tag{48a}$$

$$(D^2 + \omega^2 \lambda_y^2) V(\xi) = 0, \tag{48b}$$

$$(D^2 + \omega^2 \lambda_\varphi^2) \Phi(\xi) = 0. \tag{48c}$$

These are precisely the three governing equations of uncoupled motion previously developed from first principles in Eqs. (8) and whose exact solutions are given in dynamic stiffness terms by Eq. (20).

5.2. Coupling of the modes

A three-dimensional shear–torsion beam is now considered with three different sets of boundary conditions imposed in turn. In each case an exact relationship is developed between the coupled and uncoupled natural frequencies.

5.2.1. Free–free member

The natural frequencies of a three-dimensional, free–free member can be determined as those values of the frequency that cause the determinant of its dynamic stiffness matrix to be zero, since the boundary conditions impose no constraint on the member. Although $|\mathbf{k}| = 0$ could be solved analytically from Eq. (47), such a tedious approach is not required since identical results can be achieved by a simple alternative method based on Eq. (44) with $\mathbf{p} = \mathbf{0}$. Hence

$$\mathbf{s}^* \mathbf{c} = \mathbf{0}. \tag{49}$$

The non-trivial solutions of Eq. (49) can be obtained from

$$|\mathbf{s}^*| = 0, \tag{50}$$

where $|\mathbf{s}^*|$ is always a smooth continuous function of frequency. Substituting $\mathbf{s}^*$ from Eq. (43) into Eq. (50) gives

$$\begin{vmatrix} \mathbf{DEb} & \mathbf{0} \\ \mathbf{0} & \mathbf{DEb} \end{vmatrix} \begin{vmatrix} \mathbf{0} & -\mathbf{I} \\ -\mathbf{S} & \mathbf{C} \end{vmatrix} = 0. \tag{51}$$

Now it is easy to show that the left-hand determinant for a member with a doubly asymmetric cross-section cannot be zero for non-trivial solutions. Also, noting that the right-hand determinant is equal to $-|\mathbf{S}|$, Eq. (51) is only satisfied when the product of the diagonal terms in $\mathbf{S}$ is zero, i.e.

$$\prod_{j=1}^{3} S_{b_j\omega} = 0, \tag{52}$$

which is satisfied when

$$\left(\omega_j^{(i)} = (i-1)\frac{\pi}{b_j}, \quad j = 1,2,3\right), \quad i = 1,2,3,\ldots, \tag{53}$$

since there is a coupled frequency stemming from the ith uncoupled frequency in each of the three planes.

The natural frequencies of the analogous uncoupled free–free member, i.e. with a doubly symmetric cross-section, can easily be calculated using Eqs. (32) and (53) with $x_c = y_c = 0$. It can then be seen from Eq. (32) and the explanation below it, that the required solutions are given by

$$b^2 = -\lambda_x^2 = -b_1^2, \quad b^2 = -\lambda_y^2 = -b_2^2 \quad \text{and} \quad b^2 = -\lambda_\varphi^2 = -b_3^2, \tag{54}$$

or

$$b_1 = \lambda_x, \quad b_2 = \lambda_y \quad \text{and} \quad b_3 = \lambda_\varphi. \tag{55}$$

Hence from Eq. (53)

$$\omega_x^{(i)} = (i-1)\frac{\pi}{\lambda_x}, \quad \omega_y^{(i)} = (i-1)\frac{\pi}{\lambda_y} \quad \text{and} \quad \omega_\varphi^{(i)} = (i-1)\frac{\pi}{\lambda_\varphi}, \quad i = 1,2,3,\ldots. \tag{56a–c}$$

Premultiplying Eqs. (32) by

$$\begin{vmatrix} \dfrac{1}{b^2\lambda_x^2} & 0 & 0 \\ 0 & \dfrac{1}{b^2\lambda_y^2} & 0 \\ 0 & 0 & \dfrac{1}{b^2\lambda_\varphi^2} \end{vmatrix} \tag{57}$$

leaves the result unaltered, but enables the determinant to be written as

$$\begin{vmatrix} \dfrac{1}{\lambda_x^2} + \dfrac{1}{b^2} & 0 & -\dfrac{y_c}{b^2} \\ 0 & \dfrac{1}{\lambda_y^2} + \dfrac{1}{b^2} & \dfrac{x_c}{b^2} \\ -\dfrac{y_c}{b^2} & \dfrac{x_c}{b^2} & r_m^2\left(\dfrac{1}{\lambda_\varphi^2} + \dfrac{1}{b^2}\right) \end{vmatrix} = 0. \tag{58}$$

Since $-b_j^2$ ($j=1,2,3$) are the roots of Eq. (58), substituting $1/\lambda_x^2$, $1/\lambda_y^2$, $1/\lambda_\varphi^2$ and $1/b_j^2$ ($j=1,2,3$) from Eqs. (56) and (53) in Eq. (58) gives

$$\begin{vmatrix} \omega_j^{(i)^2}-\omega_x^{(i)^2} & 0 & -y_c\omega_j^{(i)^2} \\ 0 & \omega_j^{(i)^2}-\omega_y^{(i)^2} & x_c\omega_j^{(i)^2} \\ -y_c\omega_j^{(i)^2} & x_c\omega_j^{(i)^2} & r_m^2\left(\omega_j^{(i)^2}-\omega_\varphi^{(i)^2}\right) \end{vmatrix} = 0 \quad (j=1,2,3) \quad (i=1,2,3,\ldots). \tag{59}$$

Eq. (59) defines the exact relationship between the coupled natural frequencies of a member with a doubly asymmetric cross-section $\omega_j^{(i)}$ and the corresponding uncoupled natural frequencies in the x, y and torsional directions. Since $\omega_x^{(i)}$, $\omega_y^{(i)}$ and $\omega_\varphi^{(i)}$ are simple to calculate, it provides a significantly easier way of finding the coupled natural frequencies.

5.2.2. Clamped–clamped member

In similar fashion to the previous section, the most efficient way of determining the coupled natural frequencies is to use Eq. (40) and note that $\mathbf{d}=\mathbf{0}$ for a clamped–clamped member. The required condition is then that $|\mathbf{s}|=0$ and from Eq. (39) this is equivalent to

$$\begin{vmatrix} \mathbf{E} & \mathbf{0} \\ \mathbf{0} & \mathbf{E} \end{vmatrix} \begin{vmatrix} \mathbf{I} & \mathbf{0} \\ \mathbf{C} & \mathbf{S} \end{vmatrix} = 0. \tag{60}$$

Once more, it is easy to show that the left-hand determinant for a member with a doubly asymmetric cross-section cannot be zero for non-trivial solutions. Thus, noting that the right-hand determinant is that of a lower triangular matrix, Eq. (60) is only satisfied when the product of its significant leading diagonal terms is zero, i.e.

$$\prod_{j=1}^{3} S_{b_j\omega} = 0, \tag{61}$$

which is satisfied when

$$\left(\omega_j^{(i)} = \frac{i\pi}{b_j}, \quad j=1,2,3\right), \quad i=1,2,3,\ldots. \tag{62}$$

The natural frequencies of the analogous uncoupled clamped–clamped member can easily be calculated using Eqs. (32) and (53) with $x_c=y_c=0$. From Eq. (32) it is clear that

$$b_1=\lambda_x, \quad b_2=\lambda_y \quad \text{and} \quad b_3=\lambda_\varphi. \tag{63}$$

Hence from Eq. (62)

$$\omega_x^{(i)}=\frac{i\pi}{\lambda_x}, \quad \omega_y^{(i)}=\frac{i\pi}{\lambda_y} \quad \text{and} \quad \omega_\varphi^{(i)}=\frac{i\pi}{\lambda_\varphi}, \quad i=1,2,3,\ldots. \tag{64a–c}$$

In a similar fashion to the free–free member, the relationship between the coupled and uncoupled natural frequencies of a clamped–clamped member can be obtained by substituting $1/\lambda_x^2$, $1/\lambda_y^2$, $1/\lambda_\varphi^2$ and $1/b_j^2$ from Eqs. (64) and (62) into Eq. (58). Eq. (59) therefore provides an exact solution for clamped–clamped members too.

5.2.3. Clamped–free member

The boundary conditions for a cantilever beam that is clamped at node 1 and free at node 2 are

$$\mathbf{d}_1=\mathbf{0}; \quad \mathbf{p}_2=\mathbf{0}. \tag{65a,b}$$

Eq. (65b) can be written in the following form using Eqs. (37):

$$\begin{bmatrix} DU(\xi=1) \\ DV(\xi=1) \\ D\Phi(\xi=1) \end{bmatrix} = \mathbf{0} \quad \text{or} \quad \mathbf{d}_2' = \mathbf{0}, \tag{66}$$

where $\mathbf{d}_2'$ is the derivative of the vector of displacement components when $\xi = 1$.

If Eqs. (65a) and (66) are substituted into Eqs. (39), suitably differentiated, it is clear that the condition for non-trivial solutions is

$$b_1 b_2 b_3 \omega^3 \begin{vmatrix} \mathbf{E} & \mathbf{0} \\ \mathbf{0} & \mathbf{E} \end{vmatrix} \begin{vmatrix} \mathbf{I} & \mathbf{0} \\ \mathbf{S} & \mathbf{C} \end{vmatrix} = 0. \tag{67}$$

However, it is easy to show that only the right-hand determinant can pass through zero for non-trivial solutions. Thus, noting that it has the form of a lower triangular matrix, Eq. (67) is only satisfied when the product of its significant leading diagonal terms is zero, i.e.

$$\prod_{j=1}^{3} C_{b_j\omega} = 0, \tag{68}$$

which is satisfied when

$$\left(\omega_j^{(i)} = \left(i - \frac{1}{2}\right)\frac{\pi}{b_j}, \quad j = 1,2,3\right), \quad i = 1,2,3,\ldots. \tag{69}$$

Hence the required natural frequencies can be determined conveniently using Eqs. (69).

As before, the natural frequencies of an analogous uncoupled clamped–free member can easily be calculated using Eqs. (32) and (69), with $x_c = y_c = 0$. From Eq. (32) it is clear that

$$b_1 = \lambda_x, \quad b_2 = \lambda_y \quad \text{and} \quad b_3 = \lambda_\varphi \tag{70}$$

and hence from Eq. (68)

$$\omega_x^{(i)} = \left(i - \frac{1}{2}\right)\frac{\pi}{\lambda_x}, \quad \omega_y^{(i)} = \left(i - \frac{1}{2}\right)\frac{\pi}{\lambda_y} \quad \text{and} \quad \omega_\varphi^{(i)} = \left(i - \frac{1}{2}\right)\frac{\pi}{\lambda_\varphi}, \quad i = 1,2,3. \tag{71a–c}$$

In a similar fashion to the free–free member, the relationship between the coupled and uncoupled natural frequencies of a clamped–free member can be obtained by substituting $1/\lambda_x^2$, $1/\lambda_y^2$, $1/\lambda_\varphi^2$ and $1/b_j^2$ from Eqs. (71) and (69) into Eq. (58). Eq. (59) therefore provides an exact solution for clamped–free members as well.

5.3. Advantages of the two-dimensional approach

The two-dimensional approach offers two major advantages. Firstly, it is very much faster than using the three-dimensional equations. Secondly, it can deal with singly or doubly asymmetric sections equally easily, by setting either x_c or y_c equal to zero in Eq. (59). This is not possible with the three-dimensional equations, which have to be re-cast from first principles.

6. Numerical results

The purpose of this section is to clarify the use of the two-dimensional approach by giving two examples. The first example demonstrates the ability of the method to calculate the coupled natural frequencies of a continuous, but stepped, three-dimensional shear–torsion beam with doubly asymmetric cross-section. In the second example the theory is used efficiently to generate a comprehensive parametric study that investigates the effect of the eccentricity of the mass axis, together with the ratio of the torsional to translational rigidity, by comparing the coupled and uncoupled natural frequencies of a shear cantilever with a doubly asymmetric cross-section.

Example 1. A continuous, three dimensional, stepped, shear–torsion beam with doubly asymmetric cross-section is now considered. The structure is analysed with three sets of boundary conditions, namely clamped–clamped, clamped–free and free–free. It should be noted that the natural coupling between component members must not be destroyed. Thus a nodal support in one plane must be echoed in the other planes. The properties of each of the stepped sections are given in Fig. 5. The eccentricities and polar mass radius of gyration of the cross-section about the z-axis for all sections in the coordinate system of Fig. 1 are $x_c = 0.2\,\mathrm{m}$, $y_c = 0.3\,\mathrm{m}$ and $r_m^2 = 0.23\,\mathrm{m}^2$.

Table 1 shows the uncoupled natural frequencies for the structure of Example 1 obtained when using the appropriate form of Eq. (20) that corresponds to uncoupled motion in the x–z, y–z and torsional planes taken in turn. Table 2 gives the corresponding coupled natural frequencies using Eq. (59) and the uncoupled frequencies of Table 1. The results are in exact agreement with the coupled natural frequencies obtained

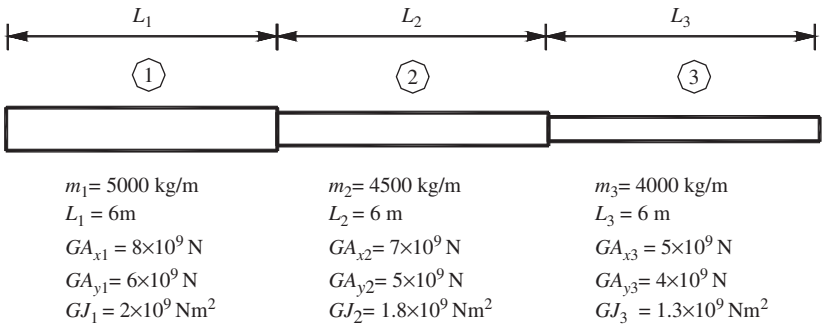

Fig. 5. Continuous stepped shear–torsion beam with doubly asymmetric cross-section.

Table 1
The uncoupled natural frequencies (Hz) of the stepped beam structure of Example 1 using the two-dimensional theory of Eq. (20) on each plane in turn

Freq. no.	x–z plane			y–z plane			Torsional		
i	C–C	C–F	F–F	C–C	C–F	F–F	C–C	C–F	F–F
1	32.23	18.40	33.93	29.14	15.84	29.21	34.97	19.31	35.85
2	67.68	50.06	66.26	58.44	43.65	57.96	71.38	52.80	69.89
3	99.76	82.42	101.27	86.95	71.59	87.78	105.35	87.00	106.67

C–F implies that the left-hand end of the structure is clamped, while the right-hand is free, etc. Rigid body modes have been omitted.

Table 2
The coupled natural frequencies (Hz) of the stepped beam structure of Example 1 derived from Eq. (59) and the uncoupled frequencies given in Table 1

Uncoupled freq. no.	$j = 1$			$j = 2$			$j = 3$		
i	C–C	C–F	F–F	C–C	C–F	F–F	C–C	C–F	F–F
1	24.90	13.68	25.29	30.59	16.78	30.95	67.40	37.20	68.85
2	50.47	37.47	49.66	61.81	45.96	60.93	137.26	101.62	134.55
3	74.70	61.62	75.59	91.55	75.51	92.67	202.62	167.31	205.28

Note that $j = 1, 2, 3$ represents the coupled frequency corresponding to the ith uncoupled frequency in the x–z, y–z and x–y (torsional) planes, respectively.

directly from the three-dimensional formulation of Eq. (47), whose development is described more fully elsewhere [25].

Example 2. The second example comprises a parametric study that illustrates the effect of both mass eccentricity and the ratio of torsional rigidity to translational rigidity on the coupled natural frequencies of a doubly asymmetric shear cantilever of constant cross-section. This particular structural form has been chosen because the non-dimensional results presented relate to any doubly asymmetric cantilever, including three-dimensional, multi-storey building structures, which can be modelled quite accurately as such [26,27].

Four non-dimensional parameters are defined, namely the ratio of torsional rigidity to translational rigidity in each plane, $\lambda_x/\lambda_\varphi$ and $\lambda_y/\lambda_\varphi$, the coupling factor, f_c, and the eccentricity ratio r_e. The coupling factor is defined as

$$f_c = \frac{(\omega_3/\omega_1)}{\max(\omega_x, \omega_y, \omega_\varphi)/\min(\omega_x, \omega_y, \omega_\varphi)}, \tag{72}$$

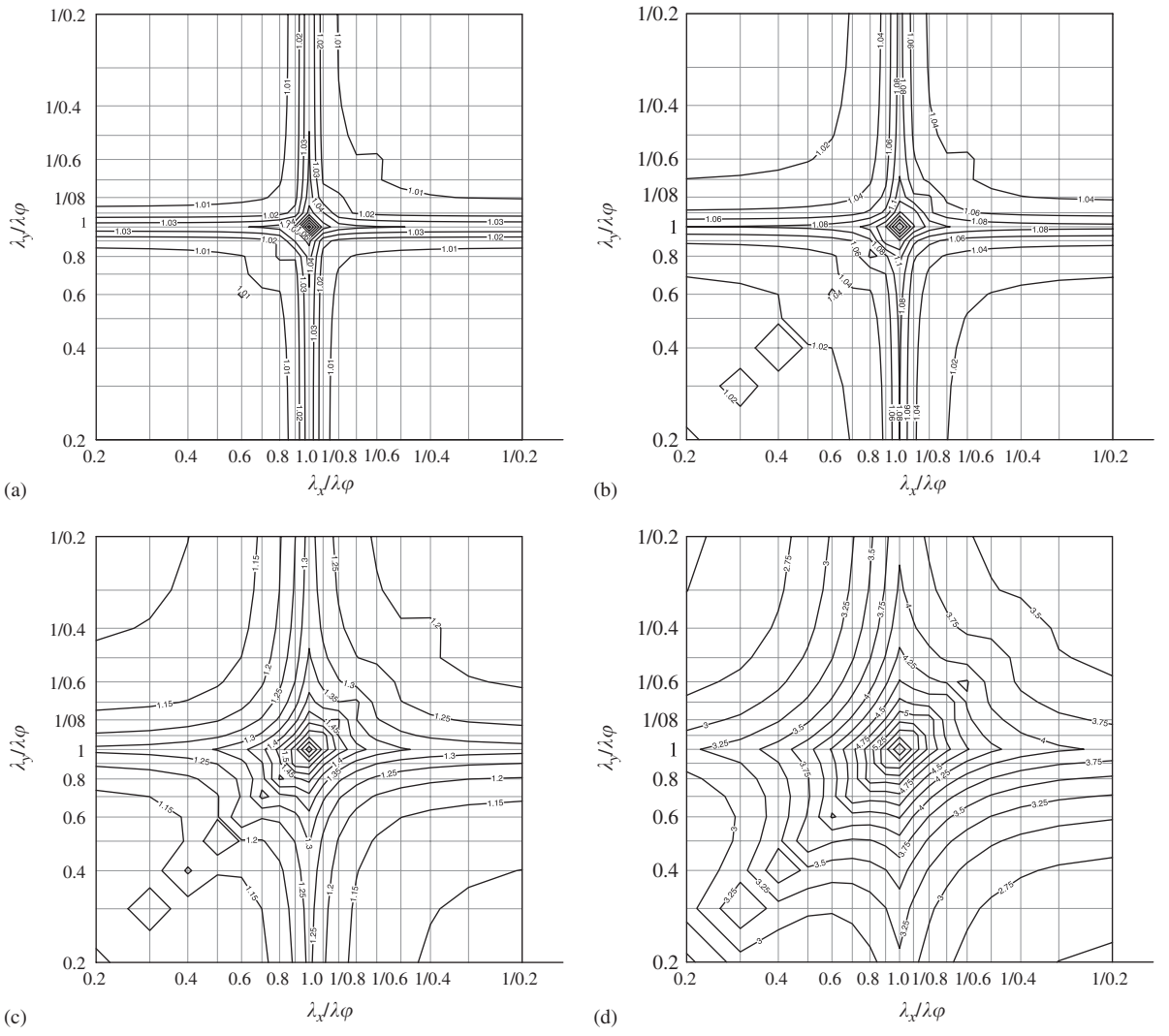

Fig. 6. Variation of the coupling factor, f_c, versus $\lambda_x/\lambda_\varphi$ and $\lambda_y/\lambda_\varphi$. f_c is shown as a set of contours that are annotated with their values where space permits. The maximum value of $f_c = f_{c\max}$ always occurs at $\lambda_x/\lambda_\varphi = \lambda_y/\lambda_\varphi = 1$. (a) $r_e = 0.1$, contour increment $= 0.01$ and $f_{c\max} = 1.10$; (b) $r_e = 0.2$, contour increment $= 0.02$ and $f_{c\max} = 1.23$; (c) $r_e = 0.5$, contour increment $= 0.05$ and $f_{c\max} = 1.73$; (d) $r_e = 0.95$, contour increment $= 0.25$ and $f_{c\max} = 6.25$.

where ω_x, ω_y and ω_φ are the fundamental uncoupled frequencies in the x–z, y–z and torsional planes and ω_1 and ω_3 are the lowest and highest frequencies of the fundamental mode of vibration. The eccentricity ratio is given as

$$r_e^2 = (x_c^2 + y_c^2)/r_m^2. \tag{73}$$

The coupling factor indicates the effect of eccentricity and the ratio of torsional rigidity to translational rigidity on the coupled frequencies, while the eccentricity parameter represents a measure of the mass centre offset from the shear centre and is equal to zero in the case of twofold symmetry. It is clear that r_e must lie in the range $0 \leqslant r_e \leqslant 1$ since $r_m^2 = r_{mc}^2 + x_c^2 + y_c^2$. The ratio of the torsional rigidity to each of the translational rigidities is assumed to vary from 0.2 to 5.

The graphs of Figs. 6a–d show the variation of f_c with $\lambda_x/\lambda_\varphi$ and $\lambda_y/\lambda_\varphi$ for $r_e = 0.1$, 0.2, 0.5 and 0.95, respectively. All necessary data to calculate the results can be inferred from the graphs.

It can be seen that maximum coupling occurs when the torsional and translational rigidities are equal. It also shows that the greater the mass centre offset, r_e, the greater the coupling factor, f_c, becomes $f_{c\max}$ shows the maximum coupling factor, f_c, for each graph. The following conclusions can also be drawn from the graphs.

1. The coupling factor, f_c, never exceeds 1.10 when $r_e \leqslant 0.1$. For such structures the effect of coupling may therefore be ignored to engineering accuracy.
2. The coupling factor, f_c, for structures in the range of $0.1 < r_e \leqslant 0.2$ is mainly smaller than 1.1. Caution should be exercised for such structures when $0.8 < \lambda_x/\lambda_\varphi < 1.25$ and $0.8 < \lambda_y/\lambda_\varphi < 1.25$.
3. For structures with $0.2 < r_e \leqslant 0.5$ the coupling factor, f_c, is generally greater than 1.10, so the effect of coupling is significant, especially if the structure's properties, $\lambda_x/\lambda_\varphi$ and $\lambda_y/\lambda_\varphi$, fall inside the contour line 1.25 in Fig. 6c.
4. The coupling factor, f_c, is quite large when $r_e = 0.95$ and it can be as big as 6.25. This shows that an offset in the mass centre may change the results by up to 600%.

7. Conclusions

A two phase process has been demonstrated that enables the coupled natural frequencies of contiguous structures composed of three-dimensional shear–torsion beams with doubly asymmetric cross-section to be determined simply and exactly using a two-dimensional approach. The solution procedure is very fast and can deal with singly or doubly asymmetric cross-sections equally easily. The method has considerable potential for modelling asymmetric three-dimensional frame structures with step changes of properties along the height of the structure.

References

[1] H.I. Laursen, R.P. Shubinski, R.W. Clough, Dynamic matrix analysis of framed structures, *Proceedings of the Fourth U.S. National Congress on Applied Mechanics*, 1962, pp. 99–105.
[2] F.Y. Cheng, Vibrations of Timoshenko beams and frameworks, *Journal of Structural Engineering—ASCE* 96 (ST3) (1970) 551–571.
[3] T.M. Wang, T.A. Kinsman, Vibration of frame structures according to the Timoshenko theory, *Journal of Sound and Vibration* 14 (1971) 215–227.
[4] W.P. Howson, F.W. Williams, Natural frequencies of frames with axially loaded Timoshenko members, *Journal of Sound and Vibration* 26 (4) (1973) 503–515.
[5] W.P. Howson, A compact method for computing the eigenvalues and eigenvectors of plane frames, *Advances in Engineering Software and Workstations* 1 (4) (1979) 181–190.
[6] W.P. Howson, J.R. Banerjee, F.W. Williams, Concise equations and program for exact eigensolutions of plane frames including member shear, *Advances in Engineering Software and Workstations* 5 (3) (1983) 137–141.
[7] W.P. Howson, A teaching analysis and design program for the complete eigensolution of plane frames using microcomputers, *International Conference on Education, Practice and Promotion of Computational Methods in Engineering using Small Computers* (*EPMESC*), Macau, 1985.
[8] F.W. Williams, D. Kennedy, Exact dynamic member stiffness for a beam on an elastic foundation, *Earthquake Engineering and Structural Dynamics* 15 (1987) 133–136.

[9] M.S. Issa, Natural frequencies of continuous curved beams on Winkler-type foundations, *Journal of Sound and Vibration* 127 (1988) 291–301.
[10] M.D. Capron, F.W. Williams, Exact dynamic stiffnesses for an axially loaded uniform Timoshenko member embedded in an elastic medium, *Journal of Sound and Vibration* 124 (3) (1988) 453–466.
[11] J.R. Banerjee, F.W. Williams, Exact Bernoulli–Euler dynamic stiffness matrix for a range of tapered beams, *International Journal for Numerical Methods in Engineering* 21 (12) (1985) 2289–2302.
[12] A.K. Gupta, W.P. Howson, Exact natural frequencies of plane structures composed of slender elastic curved members, *Journal of Sound and Vibration* 175 (2) (1994) 145–157.
[13] W.P. Howson, A.K. Jemah, J.Q. Zhou, Exact natural frequencies for out-of-plane motion of plane structures composed of curved beam members, *Computers and Structures* 55 (6) (1995) 989–995.
[14] W.P. Howson, A.K. Jemah, Exact out-of-plane natural frequencies of curved Timoshenko beams, *Journal of Engineering Mechanics—ASCE* 125 (1) (1999) 19–25.
[15] W.P. Howson, A.K. Jemah, Exact dynamic stiffness method for planar natural frequencies of curved Timoshenko beams, *Proceedings of the Institution of Mechanical Engineers Part C—Journal of Mechanical Engineering Science* 213 (7) (1999) 687–696.
[16] J.M. Gere, Y.K. Lin, Coupled vibrations of thin-walled beams of open cross-section, *Journal of Applied Mechanics* 25 (1958) 373–378.
[17] M. Falco, M. Gasparetto, Flexural-torsional vibration of thin-walled beams, *Meccanica* 8 (1973) 181–189.
[18] E. Dokumaci, An exact solution for coupled bending and torsion vibrations of uniform beams having single cross-sectional symmetry, *Journal of Sound and Vibration* 119 (3) (1987) 443–449.
[19] W.L. Hallauer, Y.L. Liu, Beam bending-torsion dynamic stiffness method for calculation of exact vibration modes, *Journal of Sound and Vibration* 85 (1) (1982) 105–113.
[20] P.O. Friberg, Coupled vibrations of beams—an exact dynamic element stiffness matrix, *International Journal for Numerical Methods in Engineering* 19 (4) (1983) 479–493.
[21] P.O. Friberg, Beam element matrices derived from Vlasovs theory of open thin-walled elastic beams, *International Journal for Numerical Methods in Engineering* 21 (7) (1985) 1205–1228.
[22] J.R. Banerjee, Coupled bending torsional dynamic stiffness matrix for beam elements, *International Journal for Numerical Methods in Engineering* 28 (6) (1989) 1283–1298.
[23] J.R. Banerjee, F.W. Williams, Coupled bending-torsional dynamic stiffness matrix for Timoshenko beam elements, *Computers and Structures* 42 (3) (1992) 301–310.
[24] J.R. Banerjee, S. Guo, W.P. Howson, Exact dynamic stiffness matrix of a bending-torsion coupled beam including warping, *Computers and Structures* 59 (4) (1996) 613–621.
[25] B. Rafezy, W.P. Howson, Exact dynamic stiffness matrix of a three-dimensional shear beam with doubly asymmetric cross-section, *Journal of Sound and Vibration* 289 (2006) 938–951.
[26] B. Rafezy, W.P. Howson, Natural frequencies of plane sway frames: an overview of two simple models, *Proceedings of ICCES 2003: International Conference on Computational and Experimental Engineering and Sciences*, Corfu, Greece, 2003, pp. 1–6.
[27] B. Rafezy, W.P. Howson, Coupled lateral–torsional vibration of asymmetric, three-dimensional frame structures, *International Journal of Solids and Structures* (2006), in press.
[28] F.W. Williams, W.H. Wittrick, Exact buckling and frequency calculations surveyed, *Journal of Structural Engineering—ASCE* 109 (1) (1983) 169–187.
[29] A.V. Balakrishnan, Generalisation of the Wittrick–Williams formula for counting modes of flexible structures, *Journal of Guidance Control and Dynamics* 18 (1995) 1410–1415.
[30] F.W. Williams, W.H. Wittrick, An automatic computational procedure for calculating natural frequencies of skeletal structures, *International Journal of Mechanical Sciences* 12 (1970) 781–791.
[31] W.H. Wittrick, F.W. Williams, A general algorithm for computing natural frequencies of elastic structures, *The Quarterly Journal of Mechanics and Applied Mathematics* 24 (3) (1971) 263–284.